School of Natural Sciences and Mathematics

2012-5-9

Low Power Greenhouse Gas Sensors for Unmanned Aerial Vehicles

Amir Khan, *et al.*

Article

Low Power Greenhouse Gas Sensors for Unmanned Aerial Vehicles

Amir Khan [1,2], **David Schaefer** [3], **Lei Tao** [1,2], **David J. Miller** [1,2], **Kang Sun** [1,2],
Mark A. Zondlo [1,2,*], **William A. Harrison** [3], **Bryan Roscoe** [3] and **David J. Lary** [3]

[1] Department of Civil and Environmental Engineering, Princeton University, Princeton, NJ 08544, USA

[2] Center for Mid-Infrared Technologies for Health and the Environment NSF-ERC, Princeton University, Princeton, NJ 08540, USA; E-Mails: makhan@princeton.edu (A.K.); ltao@princeton.edu (L.T.); djmtwo@princeton.edu (D.M.); kangsun@princeton.edu (K.S.)

[3] William B. Hanson Center for Space Science, Department of Physics, University of Texas, Dallas, TX 75080, USA; E-Mails: captdaveschaefer@gmail.com (D.S.); wah091020@utdallas.edu (W.A.H.); btr100020@utdallas.edu (B.R.); David.Lary@utdallas.edu (D.J.L.)

* Author to whom correspondence should be addressed; E-Mail: mzondlo@princeton.edu; Tel.: +1-609-258-5037; Fax: +1-609-258-2799.

Abstract: We demonstrate compact, low power, lightweight laser-based sensors for measuring trace gas species in the atmosphere designed specifically for electronic unmanned aerial vehicle (UAV) platforms. The sensors utilize non-intrusive optical sensing techniques to measure atmospheric greenhouse gas concentrations with unprecedented vertical and horizontal resolution (~1 m) within the planetary boundary layer. The sensors are developed to measure greenhouse gas species including carbon dioxide, water vapor and methane in the atmosphere. Key innovations are the coupling of very low power vertical cavity surface emitting lasers (VCSELs) to low power drive electronics and sensitive multi-harmonic wavelength modulation spectroscopic techniques. The overall mass of each sensor is between 1–2 kg including batteries and each one consumes less than 2 W of electrical power. In the initial field testing, the sensors flew successfully onboard a T-Rex Align 700E robotic helicopter and showed a precision of 1% or less for all three trace gas species. The sensors are battery operated and capable of fully automated operation for long periods of time in diverse sensing environments. Laser-based trace gas sensors for UAVs allow for high spatial mapping of local greenhouse gas

concentrations in the atmospheric boundary layer where land/atmosphere fluxes occur. The high-precision sensors, coupled to the ease-of-deployment and cost effectiveness of UAVs, provide unprecedented measurement capabilities that are not possible with existing satellite-based and suborbital aircraft platforms.

1. Introduction

The use of unmanned aerial vehicles (UAVs) for atmospheric research is rapidly growing. Their ease of deployment and high maneuverability allows them to sample areas otherwise inaccessible with conventional platforms, particularly within the planetary boundary layer of the troposphere (0.1−1 km altitude). For example, suborbital research aircraft with onboard pilots do not fly over populated areas at low altitudes, volcanoes, or into severe weather for safety reasons. Remote sensing measurements from satellite do not have the vertical or horizontal spatial resolution to identify local sources, sinks, and distributions of air pollutants and trace gases within the Earth's boundary layer. Tethered balloons and kites can provide vertical resolution measurements but only over a single location, and their deployment is limited to specific weather conditions.

UAV platforms have also demonstrated promise for atmospheric chemistry field studies. For example, UAVs have been successfully deployed over volcanoes [1] and over the Arctic Ocean sea ice [2]. A fleet of UAVs was coupled to ground-based measurements to help understand radiative heating profiles in the lower troposphere [3]. Greenhouse gas sensors have flown successfully on the NASA SIERRA Unmanned Aerial System (UAS), and novel insights into boundary layer emissions of greenhouse gases were observed (http://www.nasa.gov/centers/ames/news/releases/2011/11-45AR_prt.htm). Larger UAS, including the NASA Global Hawk, fly regular missions focusing on upper tropospheric and lower stratospheric measurements.

Substantial payloads are now routinely lifted by unmanned aerial vehicles, particularly for optical imaging. Several UAV platforms have been used in environmental applications primarily focused on geographic surveying and high-resolution temporal and spatial imaging to complement LIDAR and satellite measurements [4,5]. However, there remains a significant technology gap in the development of high-performance, high-sensitivity trace gas sensors for the more common, less expensive, and smaller UAVs that have payloads on the order of 1 kg. As such, no laser-based trace gas sensors have been developed specifically for small UAVs. Laser-based optical detection is widely used in various atmospheric, industrial and biomedical applications [6–9]. Laser-based sensors are selective, sensitive, fast, compact, and consume low power (specifically, tunable diode lasers)—essential requirements for deployment on small UAVs as well as obtaining scientifically-robust measurements.

In this study we demonstrate the development, laboratory experiments, and flight testing of novel laser-based UAV sensors for the three most important greenhouse gases: water vapor (H_2O), carbon dioxide (CO_2), and methane (CH_4). Water vapor is the most dominant greenhouse gas in the

atmosphere due to its ability to strongly absorb infrared radiation, act as a means of transfer heat from the Earth's surface to the atmosphere through latent heat of evaporation and condensation, and through cloud formation which impacts the solar and infrared radiative budgets [10–13]. Unfortunately, water vapor concentrations in the lower atmosphere can vary by nearly four orders of magnitude and show extreme heterogeneity in space and time [11]. Carbon dioxide is the most important anthropogenic greenhouse gas, but local-to-regional emissions and sinks are complicated by a lack of high spatial measurements within the boundary layer. Likewise, while the overall atmospheric budget of methane is well known, the spatial and temporal distribution of its emissions to the atmosphere are poorly constrained.

To this end we developed optical sensors which provide a compact, cost effective, fully autonomous, low-power and non-intrusive probe to measure trace gas species in the atmosphere. The measurement technique is based on laser absorption spectroscopy which uses a low power vertical cavity surface emitting laser (VCSEL) in the near-infrared spectral region. A VCSEL typically operates at 5–10 mA of current with a 5 V power supply to scan absorption features of atmospheric gaseous species of interest. The most suitable absorption line transitions available within spectral coverage of commercial VCSELs were used to maximize performance. In order to enhance the sensitivity and time response of the sensor we employ wavelength modulation spectroscopy (WMS) [9,14–17], which inherently reduces any backgrounds associated with parasitic laser scanning and modulating effects and interfering molecular transitions. For example, in a typical IR spectrum there are several regions of significant overlap from water vapor molecular transitions. These strong water vapor transitions or their line profile wing regions interfere and affect accurate measurement of gaseous species more significantly in direct absorption spectroscopy than WMS. In addition, WMS higher harmonic detection also aids in reducing interference and resolving overlapping gaseous species [18], thus providing more accurate information of the trace gas species. In addition, the combination of fast wavelength scan and modulation minimizes interference from laser $1/f_L$ noise resulting in measurements that are promising for several atmospheric sensing applications.

Robotic airborne vehicles (acrobatic helicopters and planes), when coupled with VCSEL-based sensors, allow for fast, robust, and cost-effective sampling of the atmospheric boundary layer. In this study we demonstrate the feasibility of trace gas laser-based sensors to measure greenhouse gas concentrations with high vertical and horizontal resolution within the atmospheric boundary layer. The sensors are designed for the goal of improved concentration estimates and vertical profiles of carbon dioxide, methane and water vapor (CO_2, CH_4 and H_2O), and the data will be used to model their emissions more accurately. The VCSEL-UAV sensors were successfully test-flown on a robotic helicopter (TREX Align 700E) in order to demonstrate the sensors precision, stability and performance on this unique sensing platform. The initial prototype shows short term field precision of less than 1%, mass of 2 kg, and power consumption of 2 W.

2. Sensor Design

The sensors developed for UAV applications are based on laser absorption spectroscopy. The basic sensor design includes a VCSEL (to measure CO_2, CH_4 and H_2O at 2,004 nm, 1,654 nm and 1,854 nm wavelengths, respectively), a cylindrical multi-pass cell [19] for appropriate optical

pathlength (0.1–20 m), and a 2.2 μm extended InGaAs photodetector and laser drive, detection and signal processing electronics. The WMS measurement technique has been described in detail previously [14–17]. The tunable diode laser is tuned to near an absorption line by controlling its temperature and the injected DC current. A sinusoidal modulation current (10 kHz) is introduced along with a 50 Hz sawtooth current ramp (very slow compared to the modulation frequency) which sweeps the laser wavelength across the absorption feature. The (modulated) detector signal is demodulated at fundamental and various integral multiples order of the modulation frequency—also known as phase sensitive detection. The resulting WMS signal has a derivative-like feature of the absorption lineshape profile, which attributes to the sensitivity of the measurement technique. In WMS the most common detection scheme is 2f (where f is the modulation frequency) because the 2f signals yield maximum SNR compared to higher harmonics. In our measurement scheme we used 2f and 4f detection based on optimal sensitivity of measurements. Both 2f and 4f WMS signals are symmetric and peak at the linecenter value of the absorption profile. Therefore, peak to trough height of a typical 2f signal is used to extract the information about the concentration of trace species being measured. The fundamental physical spectroscopic parameters from the HITRAN database were verified and simulated using laboratory and field measurements. This includes the collision linewidth, absorption cross-sections and lineshape function.

Optomechanically, Figure 1 shows the CO_2 sensor frame and multi-pass cell within an integrated VCSEL and photodetector on opposite ends. In general we used cylindrical, protected gold-coated mirrors of 20 cm and 50 cm focal length to obtain various optical pathlengths depending upon the species of interest. The beam from the VCSEL is highly divergent; therefore, we used a 2 μm antireflection-coated geltech-collimating lens from Lightpath Lens Technologies. A collimated beam from a VCSEL (VERTILAS, GmbH) is guided through a hole in one of the mirrors, and it is periodically reflected and refocused between the mirrors [19]. After a designated number of passes M, the beam exits through the hole (in this case from the rear mirror), in an N/2 configuration (where N is the nominal number of passes for a reentrant cylindrical pattern) and collected onto the detector. The center hole of the mirror was 3 mm in diameter, which was sufficient to channel the collimated laser beams into the multi-pass cell. The absorption pathlengths and mirror beam patterns were optimized by choosing 2f-spectra of corresponding patterns that had the least fringing and scattering from the edges of the hole of the second mirror of the multi-pass cell.

The laser was operated from a Thorlab VTC002 diode laser current driver, thermo electric cooler (TEC) module, and a custom electronic board for current sweep and modulation. The laser current ramp and sine modulator was developed using XR2206CP function generator integrated circuits. In addition, an arduino-based microcontroller was used for data and GPS logging of the sensor's flight path. The modulated signal on the photodetector (extended wavelength Indium Galium Arsenide, InGaAs, 2.2 micron (0.25 mm^2 active area) Teledyne Judson Technologies) is then demodulated at 2nd, 4th and 6th harmonic of the fundamental (modulation) frequency with a PC board lock-in amplifier (Femto Electronics—LIA BVD-150). The laser drive electronics were placed in a $20 \times 10 \times 10$ cm enclosure. The electronics board was powered using combination of Lithium polymer (LiPo) and Lithium ion batteries. The spectral data were acquired, averaged to 1 s, and recorded on a data logger (MSR 160, sample and recording rate of 1 kHz).

Figure 1. Multi-pass cell of the vertical cavity surface emitting lasers (VCSEL) sensor for atmospheric CO_2 detection. The sensor module consists of cylindrical mirrors, a VCSEL and a photodetector. The overall weight of the multi-pass cell (including the VCSEL and the detector) is less than 0.5 kg.
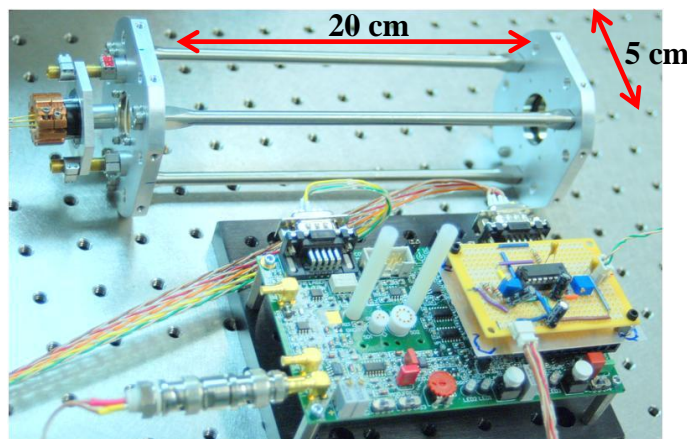
3. Laboratory Studies and Calibration

3.1. Atmospheric Trace Gas Detection

CO$_2$ detection: Atmospheric CO_2 has relatively strong absorption transitions in the IR region of the spectra where commercial VCSELs are available to probe these line transitions. For the CO_2 sensor we used a pair of 1.27 cm radius cylindrical mirrors (30 cm focal length) separated by 20 cm with 10 passes of the laser beam to yield a total absorption pathlength of 2 m in air. The VCSEL has a current tuning rate of 0.417 nm·mA^{-1} at 20 °C, which gives flexibility of a large wavelength scan. The CO_2 VCSEL can be current and temperature tuned to probe a spectral region in the range of 2001 nm to 2005 nm. Therefore, we used this VCSEL to probe atmospheric CO_2 transitions in the spectral range of 2000–2003 nm as shown in Figure 2. The figure shows numerous CO_2 and overlapping H_2O transitions in a single laser scan. The two CO_2 transitions centered at 4,994.94 cm^{-1} (2,002.02 nm) and 4,996.12 cm^{-1} (2,001.55 nm) were selected since there were no interfering H_2O absorption line transitions and their 2f-spectra were well resolved. The collision half-widths (air broadened) of each of the two CO_2 transitions are 0.072 cm^{-1} and the absorption linestrengths are of the order of 10^{-21} cm^2·molecule^{-1}·cm^{-1} for the strongest CO_2 lines and 10^{-23} cm^2·molecule^{-1}·cm^{-1} for the visible H_2O lines.

CH$_4$ detection: In order to measure atmospheric CH_4 we use a 1,654 nm VCSEL with current tuning of 0.35 nm·mA^{-1} at 20 °C. Figure 3 shows a 2f-spectrum of a laser scan probing atmospheric water vapor and methane in a single laser scan. The laser can be tuned to the isolated CH_4 absorption feature centered at 1,653.75 nm. The spectral linestrength is ~10^{-21} cm^2·molecule^{-1}·cm^{-1} with a linewidth of 0.0621 cm^{-1}. Since CH_4 absorption is relative weak at 1,653 nm range, a pathlength of 20 m yields an absorbance of the order of 10^{-3}. Therefore, we used 2.54 cm radius cylindrical mirrors with basepath of 30 cm and 60 passes of the laser beam for an optical pathlength of 18 m in air.

Figure 2. Experimental plot of a current scan of the 2,000 nm VCSEL. The plot shows 2f spectra of overlapping CO_2 and H_2O line transitions. The two CO_2 lines (shown in the highlighted region) were selected for the concentration measurements.
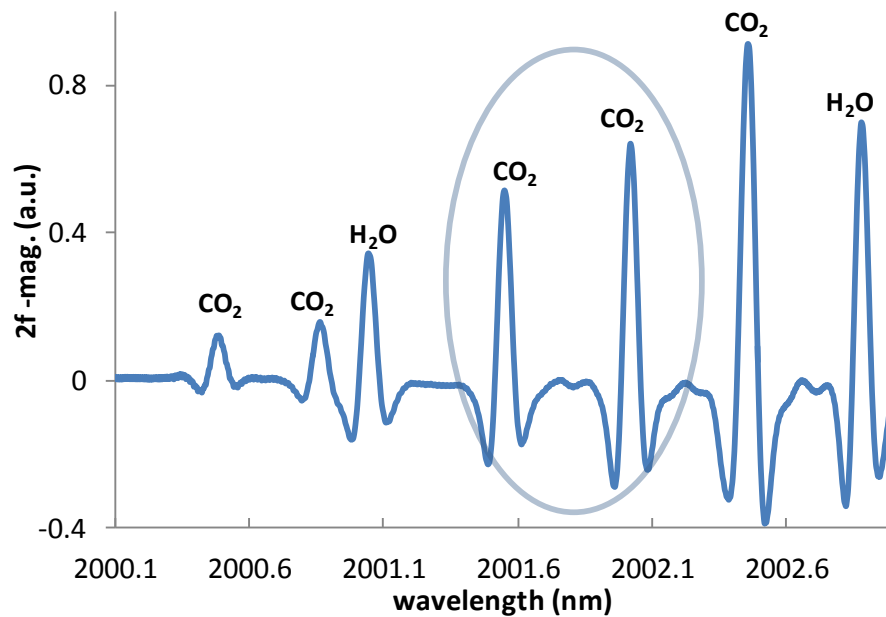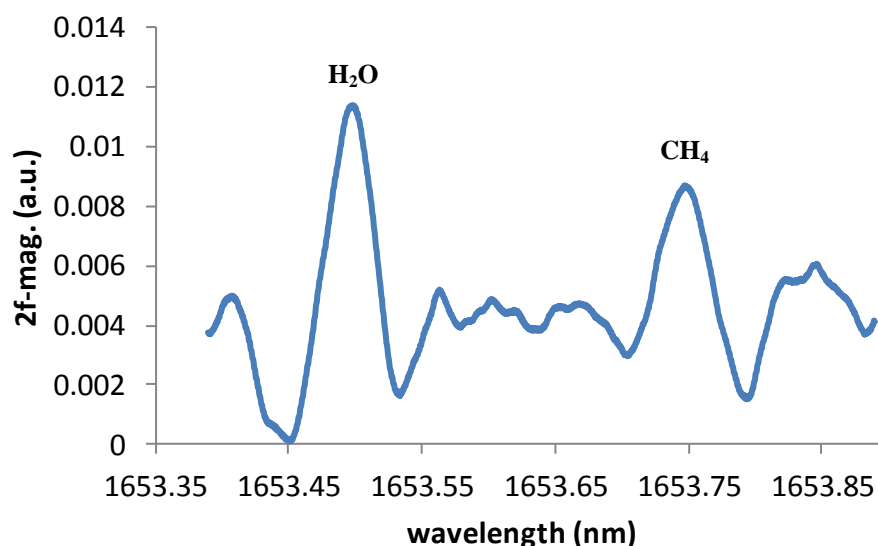

Figure 3. 2f-spectra of atmospheric CH_4 and H_2O, the height of H_2O can be used to account for humidity and water vapor correction.

H_2O detection: To measure atmospheric water-vapor we used an 1,854 nm VCSEL, which has capability of probing a strong and weaker absorption lines centered at 5,396.54 cm^{-1} (1,853.03 nm) and 5,393.65 cm^{-1} (1,854.03 nm) with spectral linestrengths of 0.996×10^{-20} cm^2 $molecule^{-1}$ cm^{-1} and 2.56×10^{-20} $cm^2 \cdot molecule^{-1} \cdot cm^{-1}$ respectively. Figure 4 shows a direct absorption and 2f-spectra of a laser scan probing these two water vapor line transitions. For this setup we did not use mirrors and instead had a simple one pass system of the laser and detector separated by 5 cm.

Figure 4. Direct absorption signal (**a**) and 2f-spectra (**b**) of a laser scan of 1,854 nm VCSEL to probe atmospheric H_2O. The spectrum shows absorption from two relatively strong molecular transitions with a very weak H_2O line transition at 1,853.37 nm. A pathlength of 5 cm gives 2% absorbance, which eliminates need of an optical multi-pass cell for this system.
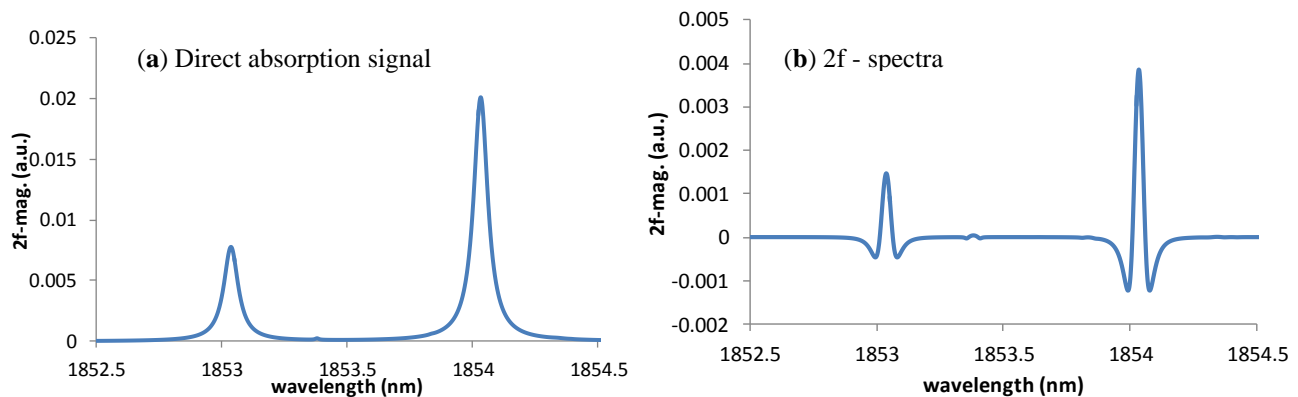

3.2. Laboratory Calibrations of VCSEL Sensors

WMS signal peak heights depend on several variables such as gas parameters (ambient temperature, pressure, concentration, lineshape function) and experimental/instrument controls (modulation amplitude, amplifier gains). These effects can be theoretically modeled by varying a parameter of interest (e.g., the density) and keeping others constant. Experimentally, these effects can complicate the measurement, but may be mitigated by utilizing optimum values of the modulation index and signal normalization techniques. We have studied these variations with numerical simulations to obtain a precise relationship between experimental variables and uncertainties and their effects on WMS signals. This requires accurate knowledge of spectroscopic parameters for absorption lines of interest, which can be theoretically modeled with experiments while incorporating known experimental sources of errors such as residual amplitude modulation effects typically found in diode laser spectroscopy. In our analysis, for simplicity, many instrumentation related parameters are not taken into account. This is because values for a number of parameters related to the instrument hardware are required, which includes the laser intensity, detector sensitivity, noise figures, lock-in amplifier gain and bandwidth, etc. The conventional approach around these issues is to calibrate the sensor at a reference condition to eliminate the dependence of hardware-related parameters. Furthermore, the 2f (or 4f) WMS signal can be normalized to 1f (or direct absorption signal), provided there is a linear laser intensity variation with the wavelength. In general, this normalization of the WMS-Nf signal with the WMS-1f signal can provide the instantaneous laser intensity.

We have adapted similar approaches to evaluate and quantify the drift and stability of the sensors. In order to evaluate stability and sources of drift in the sensor we use multiple approaches. First, due to enhanced tunability of VCSELs, all three sensors are capable of scanning multiple line transitions in a single scan. There we use two consecutive line transitions and their respective 2f and 4f signals and their ratios to normalize for the laser intensity, concentration and instrument related drifts. For example, in the CO_2 scan, one can easily probe two CO_2 line transition in a single laser scan (Figure 2). The ratio of these two line transitions can be used to investigate temperature or fringe background-related

drifts. Secondly, 4f detection provides multiple zero crossings and turnings points within a 4f-spectrum. The ratios of combinations each of these turning points, which are essentially independent of concentration or atmospheric variability of gaseous species, can be used to track drifts in the sensor. Finally, both CO_2 and CH_4 sensors are also capable of probing water vapor transitions which can be used for water vapor corrections.

All three sensors (CO_2, CH_4 and H_2O) were calibrated in the laboratory for estimation of stability and drift analysis of the instrument. Figure 5 shows Allan deviation plots of CO_2 and CH_4 for ambient atmospheric concentrations of each gas. The Allan deviation is obtained by measuring an experimental variable such as the concentration in a "stable" environment such that its value over time is held constant [20]. The Allan deviation plots are examined to study the impact of changes in the environment upon the measurement itself. For example, electronics noise, temperature cycling of the total system (which includes the electronics and optomechanical components), and variations in room temperature/pressure all affect the measurement. In these experiments, it was not possible to control the environmental temperatures and pressures and thus these values fluctuated by ambient levels (few degrees C; few hPa pressure). These results are important for a UAV sensor where significant changes in temperature are expected in vertical and horizontal profiling of the atmosphere. Allan deviation plots yield information on noise sources, the limit of signal averaging, and the extent to which long-term drift degrades the precision on longer timescales. The CO_2 sensor has shown short term laboratory precision of 0.02% with a 1 s averaging time, whereas, the CH_4 sensor has a precision of 0.05% with 1 s averaging time. It is emphasized that although our short term laboratory precision is excellent, our field precision is degraded to ~1% on timescales of minutes. Most common sources of drift are attributed to temperature response to the fringe background, laser TEC and to some extent the detection electronics.

Figure 5. Allan deviation of CO_2 (**a**) and CH_4 (**b**) sensor shows optimal averaging time and instrument noise affecting the signal and the ultimate detection limit.

(**a**)   (**b**)
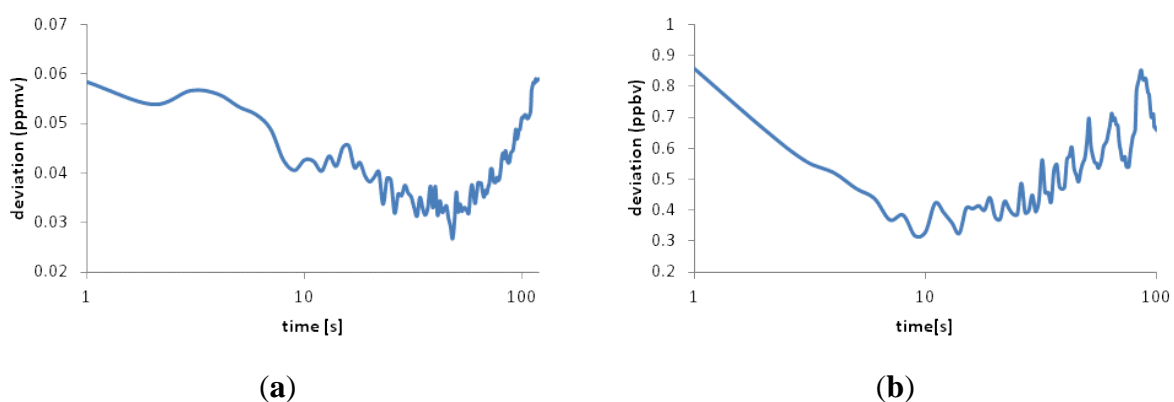
In addition to studies with Allan deviation for each sensor, the measurements from CO_2 sensor were also intercompared with a commercial LICOR (LI-7500A) NDIR based CO_2 and humidity sensor [21]. The intercomparison results are shown in Figure 6 for a twelve hour time series in the laboratory. We used both 2f and 4f-detection, however, 4f-detection showed better correlation due to greater sensitivity to a large variation in CO_2 concentration and also aids reducing signal background from Fabry-Perot fringing from the optical surfaces in the sensor. This strategy works best while probing

large dynamic range of a concentration of a gaseous species in the atmosphere. The correlation coefficient of the VCSEL CO_2 and LICOR sensor is 0.92. The correlation plot is shown as an inset in Figure 6. The mismatch between both sensors is largely attributed to gradual offsets due to ambient temperature-related drifts to the laser.

Figure 6. Sensor intercomparison: 12 h time series of ambient CO_2 detection from collocated VCSEL and LICOR (LI-7500A) sensors. The inset shows linearity between the data from the two sensors.
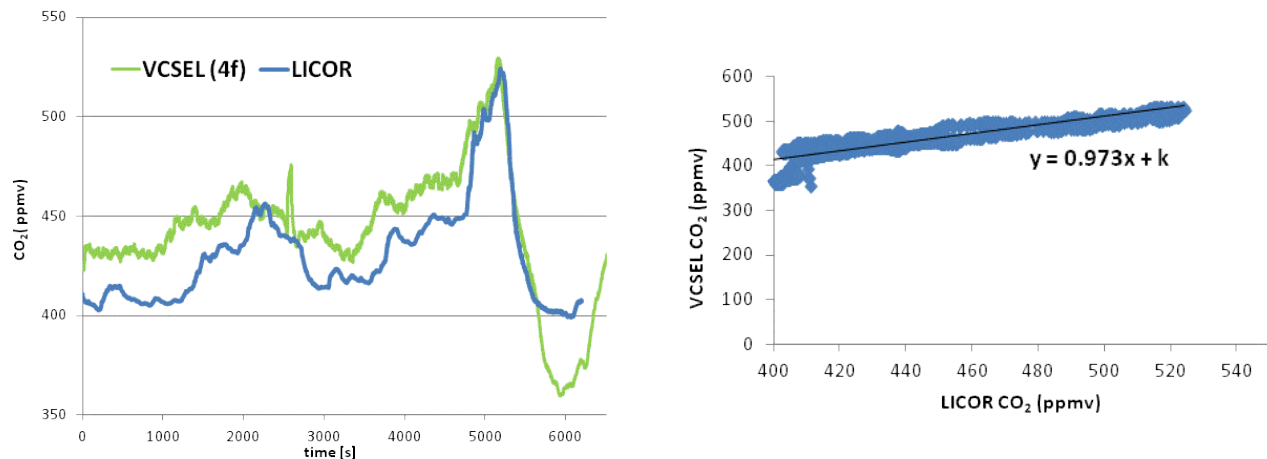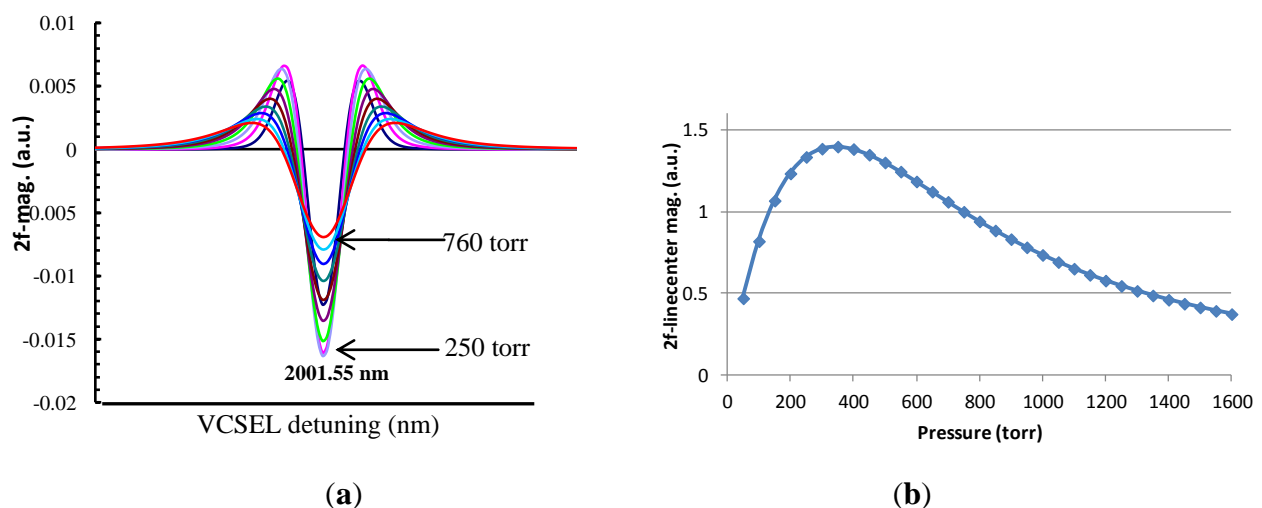

Figure 7. (**a**) Experimental 2f-spectra of a Voigt lineshape at pressures ranging from 100 Torr to 1400 Torr. (**b**) Pressure-dependence of the 2f spectra and its signal magnitude. The 2f magnitude increases with pressure (or collision width) and decreases linearly at high pressures.

(**a**)   (**b**)

Temperature and pressure corrections: Since the sensors are operated in varying altitude profiles and temperatures, one needs to account changes in environmental conditions on measurements of trace species [9,22]. In order to account for these effects, laboratory studies of a reference species is conducted and its dependence on the temperature and pressure is analyzed and compared with theoretical models. For example, Figure 7 shows the typical variation of 2f-detection spectra and signal magnitude with pressure. The functional form of these variations is incorporated in the estimation of

concentration. The 2f WMS signals are dependent on the Doppler and collision widths of the lineshape function. Currently the 2f spectra (100 Hz) points are recorded and the concentration is estimated based on these points. The sensor will be modified to log the ambient temperature and pressure during its flight path. These parameters are used to post process the spectra and apply for temperature, pressure and water vapor corrections. It is noteworthy that the changes close to ambient temperature and pressure conditions translate into less than 0.1 % change in WMS signal magnitude. Based on the current operating altitude of the prototype sensor and the limits of corresponding field precision, such effects do not reflect on the measurements.

4. UAV Specifications and Sensor Flight Tests

The overall size of each sensor is 20 cm $\times$ 5 cm $\times$ 5 cm with a mass of ~2 kg or less including batteries. The sensor is battery-operated with electrical power consumption of 2 W and capable of performing autonomous operation (trace gas WMS detection and onboard data acquisition). All sensors were test deployed on the ground at the field site, prior to their flight testing, to assess their stability and precision. In addition, additional tests were conducted prior to flight testing to ensure no significant changes occurred from the earlier laboratory results. The estimated precision for 1 s averaged data was comparable to the laboratory tests. Signal averaging improves the precision by the inverse square root of integration time up to 10 s or higher based on fringe backgrounds affecting the system.

The UAV used for flight testing was the UT-Dallas Align T-REX 700E robotic helicopter (Table 1) with payload capacity of up to 5 kg depending on the required flight durations and other payload constraints. The UAV is a flybarless acrobatic helicopter. It is 133 cm long, 41 cm high, has a main rotor diameter of 156 cm, with a flying mass excluding payload of approximately 4.7 kg. The helicopter operates with a dual 5,500 mAh LiPo battery pack and has been flown with an additional payload of 7 kg. The sensor was mounted on a bar that projects in front of the helicopter forward of the main rotor downdraft.

Table 1. Specifications of robotic helicopter used for VCSEL sensors.

| Specifications	Helicopter
Model	Align T-REX 700E V2
Payload	5 kg
Duration at Payload	20 min.
Horizontal Range	2 km (line-of-sight)
Vertical Range	0–1 km
Airspeed	0–15 m·s^{-1}
Operation	Remote-controlled
Data	Serial ports

The sensors were flown at a University of Texas at Dallas field site in Richardson, Texas. The UAV helicopter (Figure 8) was operated at airspeed of 15 m·s^{-1} to obtain greater spatial resolution than conventional aircraft sampling strategies. Figure 9 shows representative time series of vertical/spatial timeseries of CO_2, CH_4 and H_2O measurements to probe atmospheric variability of these gases. The changes observed during in-flight measurements were much greater than the sensor precision over

these durations. For the purposes of the test flights we assumed nominal atmospheric levels of the trace gas species, as full calibrations were beyond the scope of the test flights. The figure shows flat regions during flight operation which were used to estimate the short term precision of the sensor during flight. For example, the estimated in-flight precision at 1 Hz for CO_2, CH_4 and H_2O was 0.1 ppmv, 2 ppbv and 20 ppmv, respectively. The total flight duration varied from 5–10 min and over this entire duration we estimate the longer-term precision (drift) in the sensors was around 1%. The flight duration was primarily constrained by the battery capacity of the helicopter used during flight tests. During the flight test all critical sensor controls, e.g., VCSEL current, laser temperature detector dc amplitude were continuously monitored and found to be stable during the entire flight operation. Therefore, in most test flights there were no apparent electromagnetic interferences, static, or mechanical vibrational issues affecting the performance of sensors' electronics or their optomechanical alignments.

Figure 8. Robotic helicopter with VCSEL sensor onboard.

Figure 9. Atmospheric H_2O, CH_4, and CO_2 profile from a test flight of VCSEL-UAV sensor.
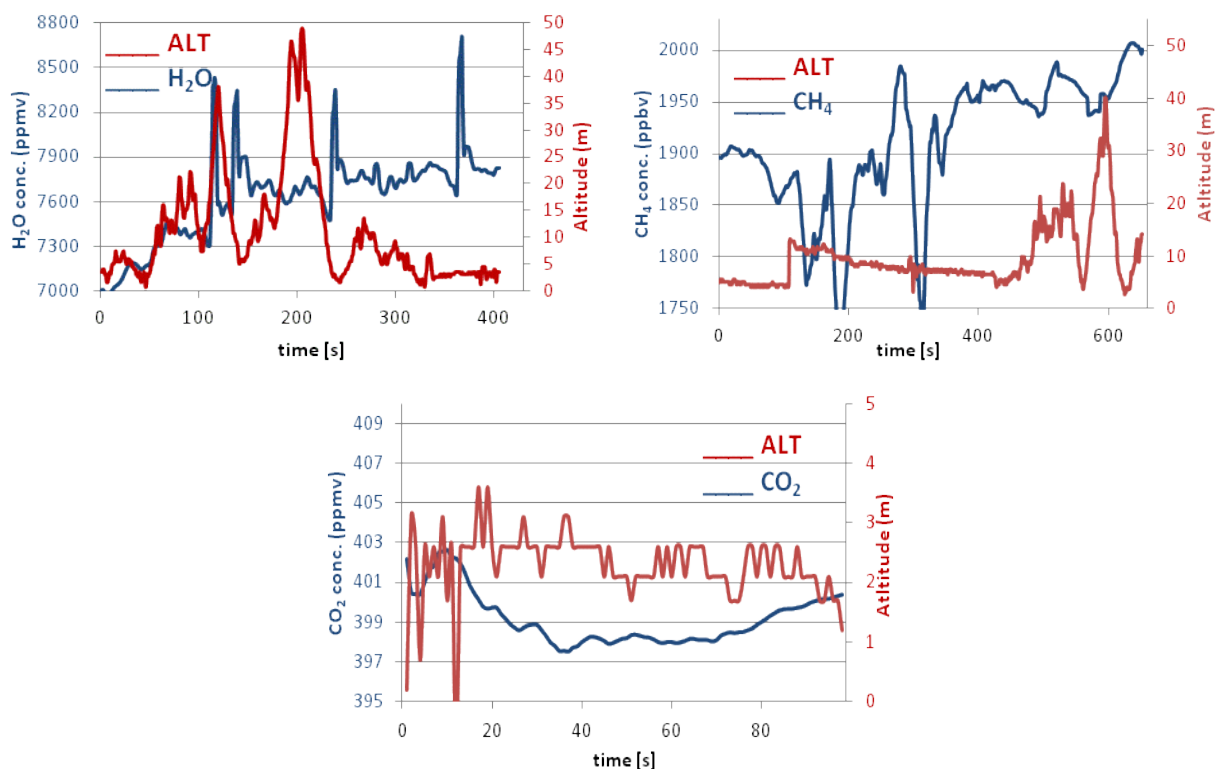
CH_4 and CO_2 are largely invariant (1–5%) in the atmosphere at levels near 1,800 ppbv and 400 ppmv, respectively. Thus, the relevant figure-of-merit for measuring these species is the precision rather than the detection limit. Both gases require precision <1% to be relevant for identifying significant local sources and sinks. In contrast, H_2O is more variable in the atmosphere, and thus the detection limit and dynamic range are more important than the precision (< 2%). Table 2 summarizes each gas in the lower troposphere (5 km) and observed measurement figures-of-merit for both laboratory as well as in-flight precision. Note that the short-term (1 Hz) in-flight precision is a worse-case scenario for precision as at least some of the variability is expected to come from real atmospheric variations. However, we again emphasize that over the course of the flight, other factors such as laser temperature stability and etalons degrade the effective precision to around 1–2% at these longer timescales.

Table 2. Mixing ratios of measured trace gases in the lower troposphere (0–5 km) and observed short-term precision over this range of the first prototype VCSEL-UAV sensors. We note that precision over timescales of the flight (5–10 min) was 1–2%.

Trace Gas	Lower Tropospheric Range	Laboratory Precision (1 Hz)	Flight Precision (1 Hz)	Mass/Power
CO_2	350–450 ppmv	0.06 ppmv	0.1 ppmv	1.5 kg/2 W
CH_4	1700–1900 ppbv	0.9 ppbv	2 ppbv	2.2 kg/2 W
H_2O	50–50,000 ppmv	<1%	20 ppmv	1 kg/2 W

5. Conclusions

The Robotic unmanned aerial vehicle (UAV) coupled with low power vertical cavity surface emitting laser (VCSEL) trace gas sensors can be an effective technology for monitoring trace species in regimes that pose challenges for aircraft and land-based atmospheric sensors. We have demonstrated compact, lightweight (1–2 kg), high-frequency (1 Hz), and cost-effective laser-based UAV sensors for high spatial (~1 m) sampling of the three most important greenhouse gases—water vapor, carbon dioxide, and methane—with flight precisions of less than 1%. Therefore, UAV trace gas sensors are ideal for mapping plumes close to the ground from a diverse variety of sources. The UAV sensors can be used for satellite validation in the atmospheric boundary layer, horizontal and vertical mapping of local pollutants and greenhouse gases, meteorology, and understanding ecosystem dynamics (e.g., carbon uptake in a forest canopy). In addition, with only slight modifications to the sensors described in this project, mid-infrared quantum cascade laser sensors can be developed to probe a larger suite of trace gas species that have higher sensitivity and selectivity in the mid-infrared spectral region [23]. Future efforts include developing an in-line reference cell and numerical algorithms to improve stability and long-term precision to levels approaching our current 1 Hz precision, increased software functionality for spectral analyses and concentration values reported in real-time, and more robust intercomparisons with other sensors. Finally, we note that the sensors, while demonstrated here on a specific robotic helicopter, are readily adaptable for use on many other UAVs and even ground-based sensor networks in remote regions where power is limited. Future plans include validation with vertical

profiles of greenhouse gases obtained from sensors on tall towers and ground-based [24], atmospheric trace gas profile networks.

References and Notes

1. McGonigle, A.J.S.; Aiuppa A.; Giudice G.; Tamburello, G.; Hodson, A.J.; Gurrieri, S. Unmanned aerial vehicle measurements of volcanic carbon dioxide fluxes. *Geophys. Res. Lett.* **2008**, *35*, L06303.
2. Curry, J.A.; Maslanik, J.M.; Holland, G.J.; Pinto, J.O. Applications of Aerosondes in the Arctic. *Bull. Am. Meteorol. Soc*. **2004**, *85*, 1855-1861.
3. Ramana, M.V.; Ramanathan, V.; Kim D.; Roberts, G.C.; Corrigan, C.E. Albedo, atmospheric solar absorption and heating rate measurements with stacked UAVs. *Q. J. R. Meteorol. Soc.* **2007**, *133*, 1913-1931.
4. Dandois, J.P.; Ellis, E.C. Remote sensing of vegetation structure using computer vision. *Remote Sens.* **2010**, *2*, 1157-1176.
5. Laliberte, A.S.; Goforth, M.A.; Steele, C.M.; Rango, A. Multispectral remote sensing from unmanned aircraft: Image processing workflows and applications for rangeland environments. *Remote Sens.* **2011**, *3*, 2529-2551.
6. Wang, C.; Sahay, P. Breath analysis using laser spectroscopic techniques: Breath biomarkers, spectral fingerprints, and detection limits. *Sensors* **2009**, *9*, 8230-8262.
7. Elia, A.; Franco, C.D.; Lugarà P.M.; Scamarcio, G. Photoacoustic spectroscopy with quantum cascade lasers for trace gas detection. *Sensors* **2006**, *6*, 1411-1419.
8. Holthoff, E.; Bender, J.; Pellegrino, P.; Fisher, A. Quantum cascade laser-based photoacoustic spectroscopy for trace vapor detection and molecular discrimination. *Sensors* **2010**, *10*, 1986-2002.
9. Asakawa, T.; Kanno, N.; Tonokura, K. Diode laser detection of greenhouse gases in the near-infrared region by wavelength modulation spectroscopy: Pressure dependence of the detection sensitivity. *Sensors* **2010**, *10*, 4686-4699.
10. Solomon, S., Qin, D., Manning, M., Marquis, M., Averyt, K., Tignor, M.M.B., Miller, H.L., Chen, Z., Eds. *Climate Change 2007: The Physical Basis*; Cambridge University Press: New York, NY, USA, 2007; p. 996.

11. Kley, D., Russell, J.M., Phillips, C., Eds. *SPARC Assessment of Upper Tropospheric and Stratospheric Water Vapor*; World Climate Research Program Reports; SPARC Office: Verrieres le Buisson Cedex, France, 2000; Volume 113, p. 324.

12. Peter, T.; Marcolli, C.; Spichtinger, P.; Corti, T.; Baker, M.B.; Koop, T. When dry air is too humid. *Science* **2006**, *314*, 1399-1402.

13. Zondlo, M.A.; Paige, M.E.; Massick, S.M.; Silver, J.A. Development, flight performance, and calibrations of the NSF Gulfstream-V vertical cavity surface emitting laser (VCSEL) hygrometer, *J. Geophys. Res.-Atmos.* **2010**, *115*, D20309.

14. Reid, J.; Labrie, D. Second-harmonic detection with tunable diode lasers—Comparison of experiment and theory. *Appl. Phys. B* **1981**, *26*, 203-210.

15. Cassidy, D.T.; Reid, J. Atmospheric pressure monitoring of trace gases using tunable diode lasers. *Appl. Opt.* **1982**, *21*, 1185-1190.

16. Bomse, D.S.; Stanton, A.C.; Silver, J.A. Frequency modulation and wavelength modulation spectroscopy: Comparison of experimental methods using a lead-salt diode laser. *Appl. Opt.* **1992**, *31*, 718-731.

17. Silver, J.A. Frequency modulation spectroscopy for trace species detection: Theory and comparison among experimental methods. *Appl. Opt.* **1992**, *31*, 707-717.

18. Dharamsi, A.N. A theory of modulation spectroscopy with applications of higher harmonic detection. *J. Phys. D* **1996**, *29*, 540-549.

19. Silver, J.A. Simple dense-pattern optical multipass cells. *Appl. Opt.* **2005**, *65*, 6545-6556.

20. Werle, P.; Mucke, R.; Slemr, F. The limits of signal averaging in atmospheric trace-gas monitoring by tunable diode laser absorption spectroscopy (TDLS). *Appl. Phys. B* **1993**, *57*,131-139.

21. *LICOR Biosciences*; http://www.licor.com/env/products/eddy_covariance/ (accessed on 29 February 2012).

22. McDermitt, D.; Burba, G.; Xu, L.; Anderson, T.; Komissarov, A.; Riensche, B.; Schedlbauer, J.; Starr, G.; Zona D.; Oechel, W. A new low-power, open-path instrument for measuring methane flux by eddy covariance. *Appl. Phys. B* **2009**, *102*, 391-405.

23. Curl, R.F.; Capasso, F.; Gmachl, C.; Kosterev, A.; McManus, B.; Lewicki, R.; Pusharsky, M.; Wysocki, G.; Tittel, F. Quantum cascade lasers in chemical physics. *Chem. Phys. Lett.* **2010**, *487*, 1-18.

24. Wunch, D.; Toon, G.C.; Wennberg, P.O.; Wofsy, S.C.; Stephens, B.B.; Fischer, M.L.; Uchino, O.; Abshire, J.B.; Bernath, P.; Biraud, S.C.; *et al*. Calibration of the Total Carbon Column Observing Network using aircraft profile data. *Atmos. Meas. Tech.* **2010**, *3*, 1351-1362.